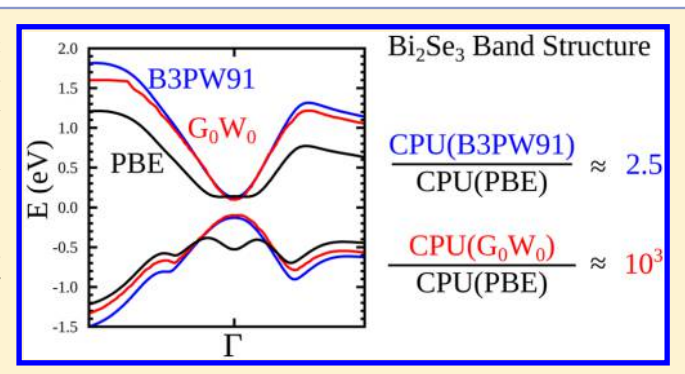# Accurate Ab Initio Quantum Mechanics Simulations of Bi_2Se_3 and Bi_2Te_3 Topological Insulator Surfaces

Jason M. Crowley, Jamil Tahir-Kheli, and William A. Goddard, III*

Materials and Process Simulation Center, MC139-74, California Institute of Technology, Pasadena, California 91125, United States

S *Supporting Information*

ABSTRACT: It has been established experimentally that Bi_2Te_3 and Bi_2Se_3 are topological insulators, with zero band gap surface states exhibiting linear dispersion at the Fermi energy. Standard density functional theory (DFT) methods such as PBE lead to large errors in the band gaps for such strongly correlated systems, while more accurate GW methods are too expensive computationally to apply to the thin films studied experimentally. We show here that the hybrid B3PW91 density functional yields GW-quality results for these systems at a computational cost comparable to PBE. The efficiency of our approach stems from the use of Gaussian basis functions instead of plane waves or augmented plane waves. This remarkable success without empirical corrections of any kind opens the door to computational studies of real chemistry involving the topological surface state, and our approach is expected to be applicable to other semiconductors with strong spin-orbit coupling.

Topological insulators are bulk insulators for which a strong spin-orbit interaction inverts the orbital character of the conduction and valence bands. In a topological insulator, there exist surface states at all energies within the bulk band gap. These surface states have a linear dispersion with respect to the surface momentum $\mathbf{k}$, and the spin polarization varies with $\mathbf{k}$.[1,2] Angle-resolved photoemission experiments on finite slabs observing the linear dispersion[3,4] show that bulk Bi_2Te_3 and Bi_2Se_3 are topological insulators.

In order to better understand the nature of these topological insulators, it is essential to determine the electronic structure. This requires an accurate prediction of band gaps (including relativistic effects) with computational efficiency sufficient for realistic surfaces and interfaces. It is generally accepted that the ideal ab initio calculation would be fully self-consistent GW[5] because it rigorously approximates the true quasiparticle energies. However, GW is computationally impractical even for bulk Bi_2Te_3 and Bi_2Se_3. A nonself-consistent GW approximation, G_0W_0, can be performed for bulk materials, but it is also impractical for slab calculations to examine the surface states. Consequently, comparisons of G_0W_0 and density functional theory (DFT) calculations on bulk solids are used to empirically correct the electronic states of the surface.[6] We refer to this approach as EC-LDA (empirically-corrected local density approximation).

DFT methods based on LDA or the generalized gradient approximation of Perdew, Burke, and Ernzerhof (PBE)[7] are practical for computation of realistic surfaces. Unfortunately, these methods underestimate band gaps in solids because of a discontinuity of the derivative of the energy with respect to the number of electrons,[8,9] the electron self Coulomb repulsion,

and the nonlinear dependence of energy on number of electrons.[10] This underestimate is especially problematic in small-gap semiconductors with strong spin-orbit coupling. Viewed as a first-order perturbation, spin-orbit coupling tends to decrease band gaps by lifting spin degeneracies in the valence and conduction bands. If the ab initio method already underestimates band gaps without spin-orbit coupling, then including it may cause an unphysical band inversion, or a "false positive" prediction that a material is a topological insulator.[11]
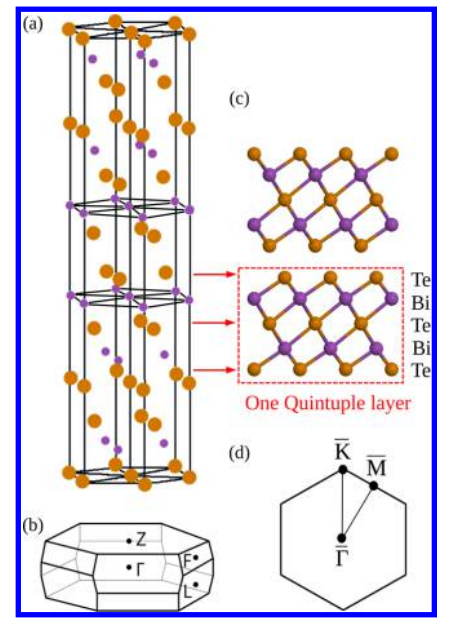
Hybrid density functionals include a fraction of exact Hartree-Fock exchange, which allows much of the self Coulomb repulsion error to be eliminated.[12] This leads to much more accurate reaction barriers so that the B3LYP hybrid method has been the *de facto* standard DFT approach in molecular computational chemistry for decades. Computing exact exchange is impractical for codes (such as VASP or Quantum Espresso) that use plane wave basis sets. This has led to increased popularity of the hybrid HSE functional,[13] which only computes the exact exchange operator over a short range. While still costly, this approach has been applied to some topological insulators using plane-wave codes.[14,15]

By contrast, with Gaussian basis sets, hybrid functionals such as B3PW91[16] (referred to as B3PW in this paper for brevity) involve computational costs comparable to PBE. We have shown elsewhere[12] that the B3PW hybrid functional used in this paper gives excellent agreement (mean absolute error =

0.09 eV) with experimental band gaps across a wide range of semiconductors.

In this paper, we show that the B3PW hybrid DFT method leads to excellent agreement with the best available G_0W_0 calculations of the bulk band structure for the topological insulators Bi_2Te_3 and Bi_2Se_3. We also report slab calculations on Bi_2Te_3 and Bi_2Se_3 using B3PW. We find that B3PW, with no empirical corrections, is in excellent agreement with the EC-LDA slab calculations. This result is the main point of our paper.

Figure 1 shows the crystal structure and Brillouin zone of bulk Bi_2Te_3 and a two quintuple layer slab. Both Bi_2Te_3 and

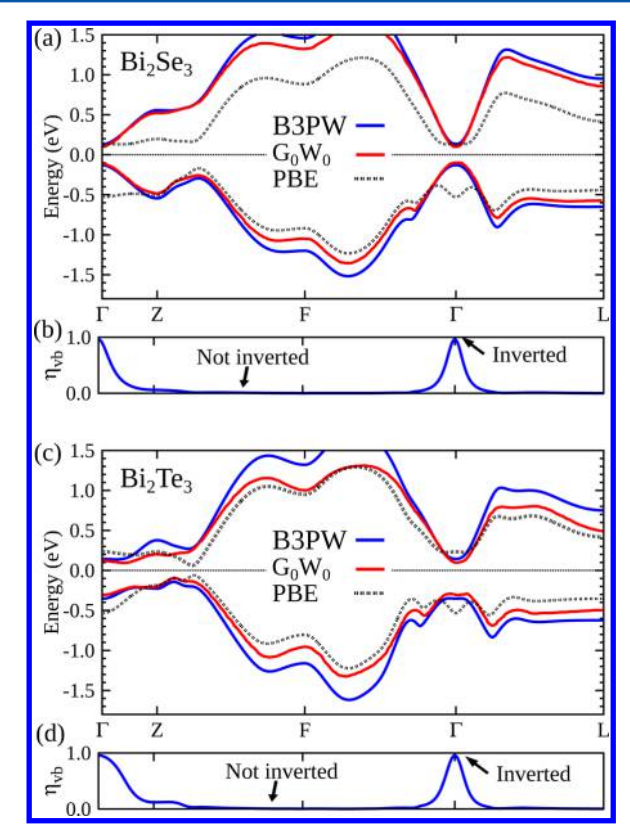
Figure 1. (a) Bulk crystal structure of Bi_2Te_3. Te and Bi atoms are colored orange and purple, respectively. (b) Bulk Brillouin zone of Bi_2Te_3 showing high-symmetry k-points. (c) Side view of a two-quintuple-layer slab of Bi_2Te_3. The red box indicates a single quintuple layer, and the arrows show the quintuple layer within the bulk structure. (d) Brillouin zone of a two-dimensional slab of Bi_2Te_3. The $\overline{\Gamma}$ point is the zone center.

Bi_2Se_3 crystallize in a layered structure composed of repeating quintuple layers (QLs). Each quintuple layer is composed of three bismuth and two tellurium layers, with the Bi and Te layers alternating. Within a QL, atoms in adjacent layers are covalently bound. In contrast, there is only van der Waals interaction between QLs.

In order to assess the quality of our hybrid approach, we compared the results of bulk band structure calculations of Bi_2Te_3 and Bi_2Se_3 with PBE and G_0W_0.[17] Our PBE calculations are in good agreement with previously published calculations.[18−20] The G_0W_0 calculation we chose for comparison was performed by Aguilera et al.[17] They used an explicitly spin-dependent G_0W_0 approximation, thereby fully accounting for the spin-orbit coupling rather than adding it as a perturbation to a scalar-relativistic calculation. The comparison is shown in Figure 2.

Physically, the most important energy regime is near the conduction and valence band edges (in the vicinity of the Γ point). Here, B3PW is in excellent agreement with G_0W_0. By contrast, PBE fails to obtain the correct band structure in the valence and conduction bands at the Γ point. In the valence

Figure 2. Comparison of the B3PW hybrid density functional (blue line) to high-quality G_0W_0 (red line) calculations of the band structures of (a) Bi_2Se_3, and (c) Bi_2Te_3. The Fermi level is set to zero. The black dashed line is the PBE result.

band for both materials, PBE always obtains a pronounced "m" shape that is not seen for Bi_2Se_3 and appears weakly for Bi_2Te_3. Additionally, B3PW and G_0W_0 predict a direct band gap for Bi_2Se_3 and an indirect gap for Bi_2Te_3 (between the Z and F points in the Brillouin zone), in agreement with recent photoemission experiments.[21,22] On the other hand, PBE finds an indirect band gap for both materials.

The excellent match we find between B3PW and the G_0W_0 valence band structure does not prove the viability of hybrid functionals. We must also ascertain whether a band inversion has occurred. Thus, we computed the degree of valence band inversion, using a previously defined expression.[6] The valence band inversion parameter, η_{vb}, is equal to one when the valence band is completely inverted. We find exactly the same inversion at the Γ point as G_0W_0, as shown in Figure 2.

Having established the accuracy of the B3PW functional for bulk band structures, we now turn to calculations for realistic slabs. A direct calculation of these slabs requires up to 35 atoms per periodic cell (whereas only 5 are required for the bulk system), making G_0W_0 impractical for the slabs. Yazyev et al.[6] empirically corrected LDA calculations to estimate G_0W_0 results for slabs (EC-LDA). In contrast, using the B3PW functional with a Gaussian basis set is quite practical for slabs.

We computed the $\overline{\Gamma}$-point band gap for slabs with 1 to 6 QLs (Figure 3) in order to determine the fewest number of quintuple layers that leads to a topological insulator. Both EC-LDA and B3PW hybrid calculations agree well with each other and the experimental results[23] for Bi_2Se_3. While the experiment found closure of the $\overline{\Gamma}$ energy gap at a minimum thickness of six QLs, both EC-LDA and B3PW did not. For B3PW, the
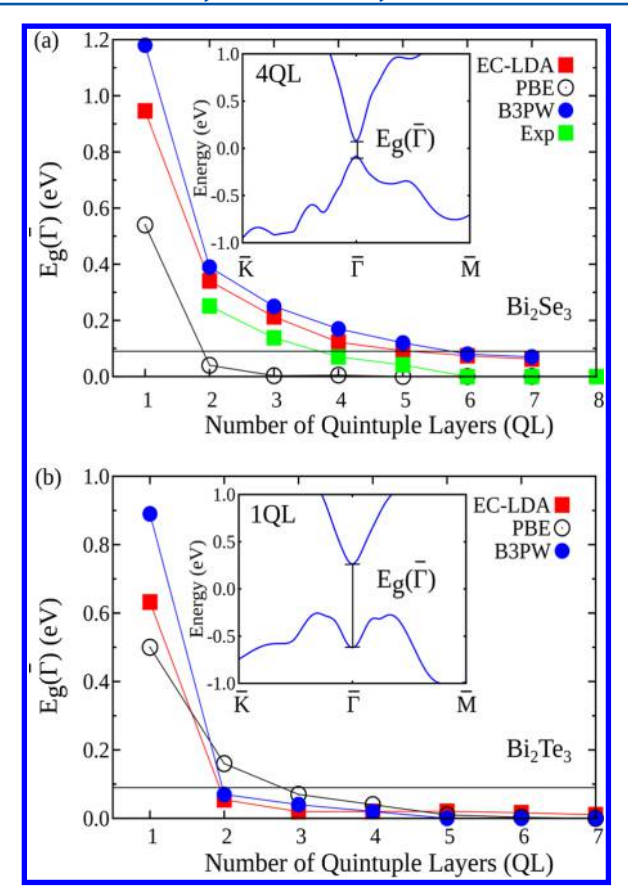
Figure 3. Comparison of our B3PW calculations (blue circles), empirically corrected LDA (EC-LDA, red squares),[6] and our PBE (open circles) calculations of the energy gap at $\bar{\Gamma}$, $E_g(\bar{\Gamma})$, for (a) Bi_2Se_3 and (b) Bi_2Te_3. The lines between the points are guides to the eye. The insets show the valence and conduction bands of (a) a four quintuple layer (4QL) slab and (b) a 1QL slab computed with B3PW. B3PW band structures for 1−7QL slabs of Bi_2Se_3 and Bi_2Se_3 are shown in the Supporting Information. The horizontal lines at 0.09 eV indicate the mean absolute error in band gaps computed with B3PW.[12] The green squares are the experimental results[23] for Bi_2Se_3. Currently, there are no experimental results for Bi_2Te_3.

mean absolute error in band gaps is known to be 0.09 eV.[12] We find band gaps below this mean absolute error for 6QL and 7QL slabs (0.08 and 0.07 eV, respectively). We believe a Dirac point exists at 6 QLs within our computational error. Our PBE calculations, as well as those of ref 24, predict zero gap by three QLs.

Relative to Bi_2Se_3, all three methods predict a faster decrease of the energy gap with film thickness in Bi_2Te_3. While the band gap is smaller than our estimated computational error by 2QLs, we see a true gap closing in Bi_2Te_3 slabs composed of five or more QLs, in contrast to EC-LDA. There is currently no experimental data for Bi_2Te_3 for QLs.

The B3PW band structures of all QL slabs for both materials are shown in the Supporting Information. There is a dramatic difference between the B3PW and EC-LDA band structures for 5QL Bi_2Te_3. The B3PW band structure has a clear Dirac cone, whereas the empirically corrected band structure of Yazyev et al.[6] does not. A true G_0W_0 calculation of a 5QL Bi_2Te_3 would most likely give a similar band structure to B3PW. Hence, we believe this is the first time an *ab initio* method has simultaneously provided accurate band gaps and demonstrated the onset of topological insulating behavior in a Bi_2Te_3 slab. At

$\bar{\Gamma}$, we find a Fermi velocity of 4×10^5 m/s, in agreement with experiment.[25]

For 5QL Bi_2Se_3, the B3PW and EC-LDA band structures are similar. Neither method predicts a Dirac point at 5QL, so in this case the Fermi velocity is zero at $\bar{\Gamma}$. Thus, we estimated the slope of the Dirac cone by fitting to the linear part of our band structure near $\bar{\Gamma}$ (0.006 to 0.05 inverse Bohr along the $\bar{M}$ direction). We find a velocity of 4×10^5 m/s, slightly below the experimental value of 5×10^5 m/s.[26]

We have shown that the hybrid B3PW functional returns GW-quality results for band gaps. We emphasize here that hybrid functionals are only practically useful for most material systems, and surfaces in particular, with the use of localized Gaussian basis sets. In order to compare the speed of calculations using Gaussians to equivalent calculations using plane waves, we performed B3LYP calculations of a 40-atom single-walled carbon nanotube system using VASP[27] version 5.2.11 and CRYSTAL09. We used 36 k-points for both calculations. The kinetic energy cutoff chosen for the VASP calculation was 400 eV; the standard 6-21G*basis set for carbon was used in CRYSTAL. Using four CPUs on exactly the same machine, VASP required 900 times more CPU time than CRYSTAL, and 9 times more memory.

With a Gaussian basis set, B3PW delivers comparable results to the highest-level G_0W_0 calculations available for significantly less cost. Indeed, this off-the-shelf functional allows direct computation of systems that are presently beyond the reach of G_0W_0. The results presented here pave the way to calculations of topological insulator surfaces and interfaces with realistic treatments of defects, doping, and surface reconstruction. All of these effects are important to accurate simulations of topological phase transitions and new spintronic devices, and our approach is expected to be effective for other semiconductors with strong spin-orbit coupling.

■ COMPUTATIONAL METHODS

Using the B3PW functional, we calculated the electronic structure of bulk Bi_2Te_3 and Bi_2Se_3 and of slabs with 1 to 6 QLs. All calculations were performed using the CRYSTAL program,[28,29] which we modified to include spin-orbit coupling. We used the fully relativistic large-core pseudopotentials and valence basis sets of Stoll et al. for Bi and Te,[30] and the small-core pseudopotential and valence basis set of Peterson et al. for Se.[31] In the valence basis sets, all exponents smaller than 0.1 were removed to ensure linear independence. A $10 \times 10 \times 10$ k-point grid was used for bulk calculations, and a $10 \times 10 \times 1$ grid was used for the slab calculations. These grids include more k-points than necessary, but the calculations are fast enough to render this overkill irrelevant. All calculations were converged to a 10^{-6} Hartree root-mean-square difference in Fock matrix elements. Convergence was accelerated using a modified Broyden approach.[32] PBE calculations were also performed using exactly the same basis sets, crystal structures, and computational parameters as our B3PW calculations in order to have a direct comparison of the results of the two functionals. For all the calculations in this paper (bulk and slabs), we find B3PW to be 2−3 times slower than an identical PBE calculation. Experimental crystal structures for Bi_2Se_3[33] and Bi_2Te_3[34] were used for both bulk and (111) slab calculations.

■ ASSOCIATED CONTENT

⑤ Supporting Information

The Supporting Information is available free of charge on the ACS Publications website at DOI: 10.1021/acs.jpclett.5b01586.

Details of the modifications to the CRYSTAL code for spin-orbit coupling and B3PW 1-7QL band structures for Bi_2Te_3 and Bi_2Se_3 (PDF)

■ AUTHOR INFORMATION

Corresponding Author
*E-mail: wag@wag.caltech.edu.

Notes

The authors declare no competing financial interest.

■ ACKNOWLEDGMENTS

■ REFERENCES

(1) Hasan, M. Z.; Kane, C. L. *Colloquium*: Topological Insulators. *Rev. Mod. Phys.* **2010**, *82*, 3045−3067.

(2) Qi, X.-L.; Zhang, S.-C. Topological Insulators and Superconductors. *Rev. Mod. Phys.* **2011**, *83*, 1057−1110.

(3) Chen, Y. L.; Analytis, J. G.; Chu, J.-H.; Liu, Z. K.; Mo, S.-K.; Qi, X. L.; Zhang, H. J.; Lu, D. H.; Dai, X.; Fang, Z.; et al. Experimental Realization of a Three-Dimensional Topological Insulator, Bi_2Te_3. *Science* **2009**, *325*, 178−181.

(4) Xia, Y.; Qian, D.; Hsieh, D.; Wray, L.; Pal, A.; Lin, H.; Bansil, A.; Grauer, D.; Hor, Y.; Cava, R.; et al. Observation of a Large-Gap Topological-Insulator Class with a Single Dirac Cone on the Surface. *Nat. Phys.* **2009**, *5*, 398−402.

(5) Hybertsen, M. S.; Louie, S. G. Electron Correlation in Semiconductors and Insulators: Band Gaps and Quasiparticle Energies. *Phys. Rev. B: Condens. Matter Mater. Phys.* **1986**, *34*, 5390−5413.

(6) Yazyev, O. V.; Kioupakis, E.; Moore, J. E.; Louie, S. G. Quasiparticle Effects in the Bulk and Surface-State Bands of Bi_2Se_3 and Bi_2Te_3 Topological Insulators. *Phys. Rev. B: Condens. Matter Mater. Phys.* **2012**, *85*, 161101.

(7) Perdew, J. P.; Burke, K.; Ernzerhof, M. Generalized Gradient Approximation Made Simple. *Phys. Rev. Lett.* **1996**, *77*, 3865−3868.

(8) Perdew, J. P.; Levy, M. Physical Content of the Exact Kohn-Sham Orbital Energies: Band Gaps and Derivative Discontinuities. *Phys. Rev. Lett.* **1983**, *51*, 1884−1887.

(9) Sham, L. J.; Schlüter, M. Density-Functional Theory of the Energy Gap. *Phys. Rev. Lett.* **1983**, *51*, 1888−1891.

(10) Mori-Sánchez, P.; Cohen, A. J.; Yang, W. Localization and Delocalization Errors in Density Functional Theory and Implications for Band-Gap Prediction. *Phys. Rev. Lett.* **2008**, *100*, 146401.

(11) Vidal, J.; Zhang, X.; Yu, L.; Luo, J.-W.; Zunger, A. False-Positive and False-Negative Assignments of Topological Insulators in Density Functional Theory and Hybrids. *Phys. Rev. B: Condens. Matter Mater. Phys.* **2011**, *84*, 041109.

(12) Xiao, H.; Tahir-Kheli, J.; Goddard, W. A. Accurate Band Gaps for Semiconductors from Density Functional Theory. *J. Phys. Chem. Lett.* **2011**, *2*, 212−217.

(13) Heyd, J.; Scuseria, G. E.; Ernzerhof, M. Hybrid Functionals Based on a Screened Coulomb Potential. *J. Chem. Phys.* **2003**, *118*, 8207−8215.

(14) Sa, B.; Zhou, J.; Sun, Z.; Tominaga, J.; Ahuja, R. Topological Insulating in $GeTe/Sb_2Te_3$ Phase-Change Superlattice. *Phys. Rev. Lett.* **2012**, *109*, 096802.

(15) Yan, B.; Jansen, M.; Felser, C. A Large-Energy-Gap Oxide Topological Insulator Based on the Superconductor $BaBiO_3$. *Nat. Phys.* **2013**, *9*, 709−711.

(16) Becke, A. D. Density-Functional Thermochemistry. III. The Role of Exact Exchange. *J. Chem. Phys.* **1993**, *98*, 5648−5652.

(17) Aguilera, I.; Friedrich, C.; Blügel, S. Spin-Orbit Coupling in Quasiparticle Studies of Topological Insulators. *Phys. Rev. B: Condens. Matter Mater. Phys.* **2013**, *88*, 165136.

(18) Wang, G.; Cagin, T. Electronic Structure of the Thermoelectric Materials Bi_2Te_3 and Sb_2Te_3 from First-Principles Calculations. *Phys. Rev. B: Condens. Matter Mater. Phys.* **2007**, *76*, 075201.

(19) Zhang, H.; Liu, C.-X.; Qi, X.-L.; Dai, X.; Fang, Z.; Zhang, S.-C. Topological Insulators in Bi_2Se_3, Bi_2Te_3, and Sb_2Te_3 with a Single Dirac Cone on the Surface. *Nat. Phys.* **2009**, *5*, 438−442.

(20) Luo, X.; Sullivan, M. B.; Quek, S. Y. First-Principles Investigations of the Atomic, Electronic, and Thermoelectric Properties of Equilibrium and Strained Bi_2Se_3 and Bi_2Te_3 Including van der Waals Interactions. *Phys. Rev. B: Condens. Matter Mater. Phys.* **2012**, *86*, 184111.

(21) Michiardi, M.; Aguilera, I.; Bianchi, M.; de Carvalho, V. E.; Ladeira, L. O.; Teixeira, N. G.; Soares, E. A.; Friedrich, C.; Blügel, S.; Hofmann, P. Bulk Band Structure of Bi_2Te_3. *Phys. Rev. B: Condens. Matter Mater. Phys.* **2014**, *90*, 075105.

(22) Nechaev, I. A.; Hatch, R. C.; Bianchi, M.; Guan, D.; Friedrich, C.; Aguilera, I.; Mi, J. L.; Iversen, B. B.; Blügel, S.; Hofmann, P.; et al. Evidence for a Direct Band Gap in the Topological Insulator Bi_2Se_3 from Theory and Experiment. *Phys. Rev. B: Condens. Matter Mater. Phys.* **2013**, *87*, 121111.

(23) Zhang, Y.; He, K.; Chang, C.-Z.; Song, C.-L.; Wang, L.-L.; Chen, X.; Jia, J.-F.; Fang, Z.; Dai, X.; Shan, W.-Y.; et al. Crossover of the Three-Dimensional Topological Insulator Bi_2Se_3 to the Two-Dimensional Limit. *Nat. Phys.* **2010**, *6*, 584−588.

(24) Yazyev, O. V.; Moore, J. E.; Louie, S. G. Spin Polarization and Transport of Surface States in the Topological Insulators Bi_2Se_3 and Bi_2Te_3 from First Principles. *Phys. Rev. Lett.* **2010**, *105*, 266806.

(25) Qu, D.-X.; Hor, Y.; Xiong, J.; Cava, R.; Ong, N. Quantum Oscillations and Hall Anomaly of Surface States in the Topological Insulator Bi_2Te_3. *Science* **2010**, *329*, 821−824.

(26) Xia, Y.; Hsieh, D.; Wray, L.; Pal, A.; Lin, H.; Bansil, A.; Grauer, D.; Hor, Y.; Cava, R.; Hasan, M. Observation of a Large-Gap Topological-Insulator Class with a Single Dirac Cone on the Surface. *Nat. Phys.* **2009**, *5*, 398−402.

(27) Kresse, G.; Furthmüller, J. Efficient Iterative Schemes for *Ab Initio* Total-Energy Calculations Using a Plane-Wave Basis Set. *Phys. Rev. B: Condens. Matter Mater. Phys.* **1996**, *54*, 11169−11186.

(28) Dovesi, R.; Orlando, R.; Erba, A.; Zicovich-Wilson, C.; Civalleri, B.; Casassa, S.; Maschio, L.; Ferrabone, M.; De La Pierre, M.; D'Arco, P.; et al. CRYSTAL14: A Program for the *Ab Initio* Investigation of Crystalline Solids. *Int. J. Quantum Chem.* **2014**, *114*, 1287−1317.

(29) Dovesi, R.; Saunders, V.; Roetti, C.; Orlando, R.; Zicovich-Wilson, C.; Pascale, F.; Civalleri, B.; Doll, K.; Harrison, N.; Bush, I. et al. *CRYSTAL14 User's Manual*; University of Torino: Torino, 2014.

(30) Stoll, H.; Metz, B.; Dolg, M. Relativistic Energy-Consistent Pseudopotentials−Recent Developments. *J. Comput. Chem.* **2002**, *23*, 767−778.

(31) Peterson, K. A.; Figgen, D.; Goll, E.; Stoll, H.; Dolg, M. Systematically Convergent Basis Sets with Relativistic Pseudopotentials. II. Small-Core Pseudopotentials and Correlation Consistent Basis Sets for the Post-d Group 16−18 Elements. *J. Chem. Phys.* **2003**, *119*, 11113−11123.

(32) Johnson, D. D. Modified Broyden's Method for Accelerating Convergence in Self-Consistent Calculations. *Phys. Rev. B: Condens. Matter Mater. Phys.* **1988**, *38*, 12807−12813.

(33) Pérez Vicente, C.; Tirado, J. L.; Adouby, K.; Jumas, J. C.; Touré, A. A.; Kra, G. X-ray Diffraction and ^{119}Sn Mössbauer Spectroscopy Study of a New Phase in the Bi_2Se_3-SnSe System: $SnBi_4Se_7$. *Inorg. Chem.* **1999**, *38*, 2131−2135.

(34) Feutelais, Y.; Legendre, B.; Rodier, N.; Agafonov, V. A Study of the Phases in the Bismuth - Tellurium system. *Mater. Res. Bull.* **1993**, *28*, 591−596.